

Organic & Biomolecular Chemistry

Accepted Manuscript



This article can be cited before page numbers have been issued, to do this please use: X. Z. Zhou, T. Liu, G. Wu, D. Kang, Z. Fu, Z. Wang, E. De Clercq, C. Pannecouque, P. Zhan and X. Liu, *Org. Biomol. Chem.*, 2019, DOI: 10.1039/C9OB00032A.



This is an Accepted Manuscript, which has been through the Royal Society of Chemistry peer review process and has been accepted for publication.

Accepted Manuscripts are published online shortly after acceptance, before technical editing, formatting and proof reading. Using this free service, authors can make their results available to the community, in citable form, before we publish the edited article. We will replace this Accepted Manuscript with the edited and formatted Advance Article as soon as it is available.

You can find more information about Accepted Manuscripts in the [author guidelines](#).

Please note that technical editing may introduce minor changes to the text and/or graphics, which may alter content. The journal's standard [Terms & Conditions](#) and the ethical guidelines, outlined in our [author and reviewer resource centre](#), still apply. In no event shall the Royal Society of Chemistry be held responsible for any errors or omissions in this Accepted Manuscript or any consequences arising from the use of any information it contains.

Targeting the hydrophobic channel of NNIBP: Discovery of novel 1,2,3-triazole-derived diarylpyrimidines as novel HIV-1 NNRTIs with high potency against wild-type and K103N mutant virus

Zhongxia Zhou,¹ Tao Liu,¹ Gaochan Wu,¹ Dongwei Kang,¹ Zhipeng Fu,¹ Zhao Wang,¹ Erik De Clercq,² Christophe Pannecouque,^{2,*} Peng Zhan,^{1,*} and Xinyong Liu^{1,*}

¹Department of Medicinal Chemistry, Key Laboratory of Chemical Biology (Ministry of Education), School of Pharmaceutical Sciences, Shandong University, 44 West Culture Road, 250012 Jinan, Shandong, PR China

²Rega Institute for Medical Research, K.U.Leuven, Minderbroedersstraat 10, B-3000 Leuven, Belgium

Abstract:

Enlightened by our previous efforts to modify diarylpyrimidines as HIV-1 non-nucleoside reverse transcriptase (RT) inhibitors (NNRTIs) and the reported crystallographic studies, we designed and synthesized novel 1,2,3-triazole-derived diarylpyrimidine derivatives *via* CuAAC "click reaction", to make additional interactions with the hydrophobic channel in the NNRTI binding pocket. The newly synthesized compounds were evaluated for anti-HIV potency in MT-4 cells. All the compounds showed favorable activity against wild-type HIV-1 strain with EC₅₀ of 0.013-5.62 μM. Interestingly, some compounds displayed remarkable potency inhibiting K103N mutant virus, a key drug-resistant mutant to the NNRTIs. Among them, *meta*-methylbenzoate (**ZL2**, EC_{50(IIB)}=0.020 μM, EC_{50(K103N)} = 0.043 μM, CC₅₀ > 241.52 μM), *para*-methylbenzoate (**ZL3**, EC_{50(IIB)} = 0.013 μM, EC_{50(K103N)} = 0.022 μM, CC₅₀ > 241.52 μM) and *para*-phenol (**ZL7**, EC_{50(IIB)} = 0.014 μM, EC_{50(K103N)} = 0.054 μM, CC₅₀ = 2.1 μM) derivatives are the three most promising compounds which are superior to the first-line antiretroviral drug efavirenz (EC_{50(IIB)} = 0.003 μM, EC_{50(K103N)} = 0.11 μM, CC₅₀ >6.34 μM) against K103N mutant strain. More encouragingly, **ZL2** and **ZL3** exhibited much lower cytotoxicity and high selection

index of >10,000 compared with all the control drugs (AZT, 3TC, NVP, EFV, ETV).
Detailed structure-activity relationship (SAR), enzymatic inhibitory activity and docking study of the representative compounds are also discussed. Furthermore, the preliminary physicochemical properties and the early metabolic stability of representative compounds were examined to evaluate their drug-like properties.

KEYWORDS: HIV-1; NNRTIs; triazole; click chemistry; diarylpyrimidines; hydrophobic channel.

1. Introduction

HIV-1 non-nucleoside reverse transcriptase (RT) inhibitors (NNRTIs) are essential components of highly active antiretroviral therapy (HAART) due to its good tolerability and low toxicity.¹⁻⁴ The non-competitive binding of NNRTIs with an allosteric site (non-nucleoside inhibitors binding pocket, NNIBP) in HIV-1 RT induces conformational changes of the catalytic active site and finally leads to inhibitory of DNA polymerase activity.⁵ There are currently six approved drugs that target the NNIBP. Nevirapine (NVP), delavirdine (DLV) are considered first generation NNRTIs and show a dramatic loss of activity with single mutations in the NNIBP. Efavirenz (EFV) is effective against many mutations except for two of the most prevalent NNRTI resistance-associated mutations, K103N and Y181C.⁶ The second-generation NNRTIs contain etravirine (ETV) and rilpivirine (RPV), belonging to diarylpyrimidine (DAPY) NNRTIs, possess broad-spectrum of anti-viral activity against clinically relevant HIV-1 mutant strains and are considered to be the most successful NNRTIs currently.⁷ Recently, a new NNRTI, doravirine was approved in the United States. However, because of the high mutation rate of HIV-1 RT and the lack of intrinsic exonucleolytic proofreading activity, new resistance strains with reduced susceptibility to ETV and RPV have emerged and are also being observed in patients.^{8,9} In addition, adverse effects such as hepatotoxicity, severe rash and central nervous system side effects appeared successively in clinical application.¹⁰

Consequently, novel NNRTI drugs with different molecular scaffolds and high potency are still needed to overcome current drug resistance regimes and adverse effects associated with the second-generation NNRTI-based anti-HIV drugs.¹¹⁻¹³

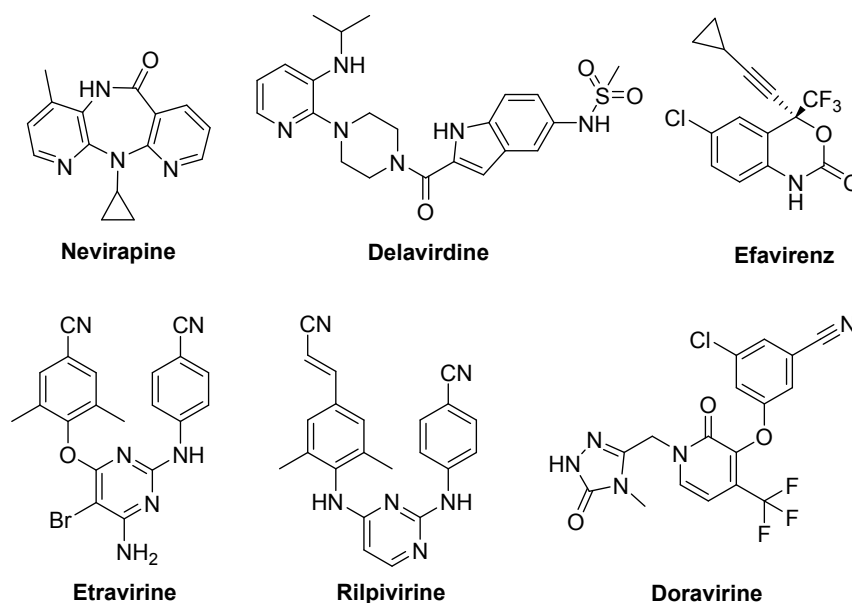


Figure 1. Chemical structures of NNRTIs approved by the U.S. FDA.

The binding mode of RPV with the NNIBP in RT is well described by the crystallography studies^{6,14}: the central pyrimidine ring and the NH linker connecting to its 2-position form two hydrogen bonds with the chain of K101; two aromatic wings of the molecule fit into two adjacent grooves composed mainly of lipophilic amino acid residues; the acrylonitrile protrudes through an opening hydrophobic channel formed by residues W229, Y188, F227, and L234.⁶ Thereinto, W229, F227, L234 were identified as highly conserved amino acids among those lining the NNIBP. Especially, it was never been observed that the mutation of the key W229 in combination with other mutations, suggesting that compensatory mutations to restore RT activity of the W229 mutated enzyme will not easily occur.⁶ The discovery of some highly conserved residues in the NNIBP opens up the possibility of finding inhibitors of anti-HIV-1 mutant strains and furnishes useful information for the rational design of new anti-HIV drugs.^{15,16} Accordingly, we focused our efforts mainly on identifying those structural requirements responsible for high activity toward an extensive range of HIV-1 variants in order to develop potential drugs with improved resistance profiles for chronic use in anti-HIV combination therapy. The

design approach discussed in this paper was mainly based on the assumption that targeting the conserved residues in the hydrophobic channel for more extensive interactions can lead to discover effective NNRTI with less sensitivity to resistance mutations.¹⁷

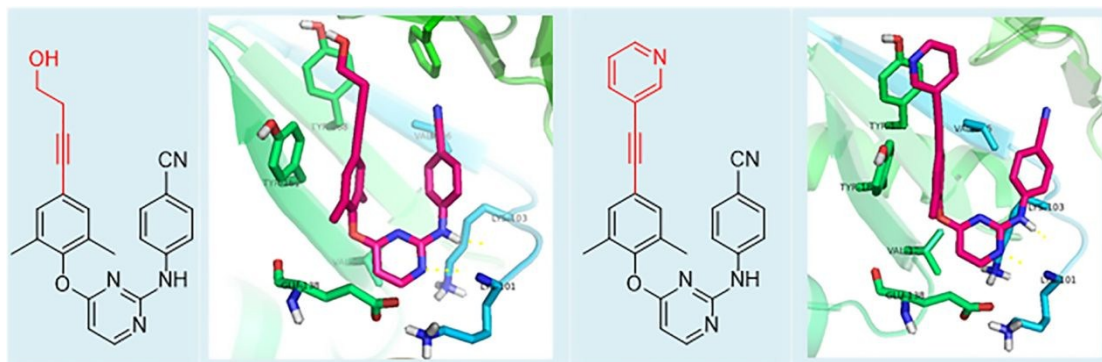


Figure 2. The binding modes of **Z10** and **Z13** (Our previous work).

In our previous work, we have conducted a preliminary exploration of the conserved amino acids in the hydrophobic channel of the NNIBP.¹⁸ In addition, two compounds, **Z10** and **Z13** turned out to be the most potent HIV-1 inhibitors with the same EC_{50} value of 3.0 nM against wild-type (WT) HIV-1 strain (**Figure 2**). Docking studies indicated that the substituted alkyne group (red) in the left wing of the inhibitors could extend to protein-solvent interface by the hydrophobic channel of NNIBP. Inspired by this, we recognized that the hydrophobic channel represented an area that had remained largely unexplored, thus, it makes sense to further explore the structure-activity relationship on the left-wing. Unique properties of 1,2,3-triazole, such as rigidity, stability and good solubility *in vivo*, hydrogen bonding capability, and dipole moment, are considered as decisive factors for their improved biological activity. For example, some 1,2,3-triazoles synthesized in our group showed a broad spectrum of antiviral activities.¹⁹⁻²² Due to the importance and implementability of 1,2,3-triazole compounds, the triazole was used as a linker in the structure to provide potential additional interactions with the surrounding residues^{6,23} (**Figure 3**). Besides, the application of the Cu(I)-catalyzed azide and alkyne 1,3-dipolar cycloaddition (CuAAC), commonly known as the "click reaction", a powerful and versatile synthetic tool in medicinal chemistry, make it easy to form the 1,4-disubstituted triazole ring.²⁰ The newly designed compounds were then synthesized and evaluated

for their anti-HIV activities against WT and multiple mutant strains. These synthetic compounds were also tested for their ability to inhibit the RT of HIV-1. Besides, the preliminary physicochemical properties and the early metabolic stability of representative compounds were examined to evaluate their drug-like properties. Herein, the result of evaluation, preliminary structure-activity relationships (SARs), modeling analysis and the drug-like properties of the most potent inhibitors will be discussed in this article.

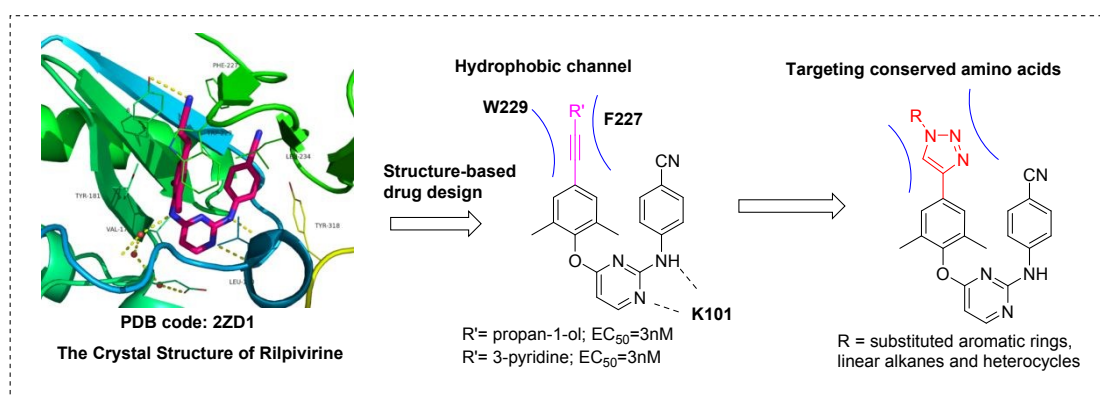
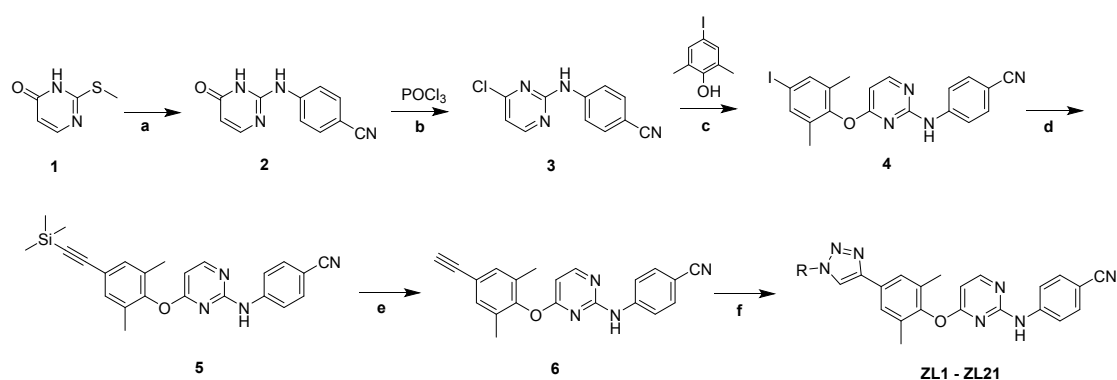


Figure 3. Illustration of the chemical modification strategy and structures of the newly designed DAPY derivatives in this study.

2. Results and discussion

2.1. Chemistry

Scheme 1. The synthetic route of 1,2,3-triazole-derived diarylpyrimidines.



Reagents and conditions: (a) 4-aminobenzonitrile, 180°C, 8h; (b) POCl₃, reflux, 0.5h; (c) K₂CO₃, DMF, 100°C, 10h; (d) Trimethylsilylacetylene, bis(triphenylphosphine)palladium dichloride, cuprous iodide, triethylamine, THF, 25°C, 10h. (e) NaOH, MeOH, rt; (f) CuSO₄·5H₂O, L-ascorbic acid sodium salt,

THF/H₂O (V:V = 1:1), rt, 4-6 h.

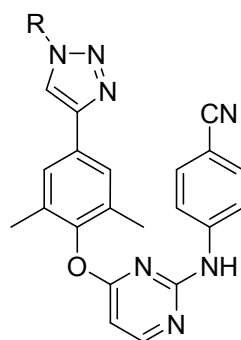
View Article Online
DOI: 10.1039/C9OB00032A

The general synthetic steps adopted to obtain the target compounds **ZL1~21** were straightforwardly outlined in **Scheme 1**. These target compounds were synthesized from the commercially available starting material 2-(methylthio)pyrimidin-4(3*H*)-one (**1**). Firstly, **1** was reacted with 4-aminobenzonitrile at 180°C by melting method to afford intermediate 4-((4-oxo-1,4-dihydropyrimidin-2-yl)amino) benzonitrile (**2**) which followed by chlorination with POCl₃ to generate 4-((4-chloropyrimidin-2-yl)amino)-benzonitrile (**3**).²⁴ Secondly, 4-iodo-2,6-dimethylphenol pass nucleophilic substitution reactions with intermediate **3** in the presence of K₂CO₃ and DMF afforded 4-((4-(4-iodo-2,6-dimethylphenoxy)pyrimidin-2-yl)amino)benzonitrile (**4**).²⁵ Thirdly, intermediate **4** underwent sonogashira coupling reaction with trimethylsilylacetylene, catalyzed by cuprous iodide, trimethylamine and bis(triphenylphosphine)palladium(II) dichloride in anhydrous THF and oxygen-free conditions to provide 4-((4-(2,6-dimethyl-4-((trimethylsilyl)ethynyl)phenoxy)pyrimidin-2-yl)amino)benzonitrile (**5**).¹⁸ De-trimethylsilane with NaOH at room temperature in methanol afforded the 4-((4-(4-ethynyl-2,6-dimethylphenoxy)pyrimidin-2-yl)amino)benzonitrile (**6**).²⁶ Then the desired compounds were generated by CuAAC “click chemistry” reaction between the substituted-azides and intermediate **6**.

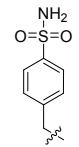
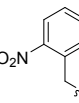
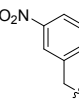
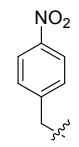
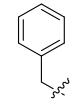
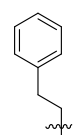
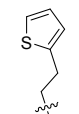
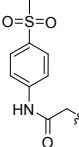
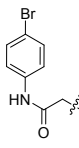
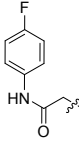
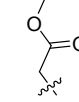
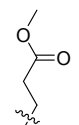
2.2. Biological activity

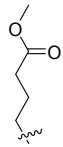
The distinct synthesized DAPYs derivatives were evaluated for their anti-HIV activities in MT4 cell against WT HIV-1 strain (IIIB), a panel of NNRTIs resistant strains with five single mutations (L100I, K103N, E138K, Y181C, Y188L) and two double mutations (K103N/Y181C (RES056) and F227L/V106A) in RT respectively. Besides, the inhibitory activity against HIV-2 strain (ROD) was also evaluated to test the selectivity of these NNRTIs, and zidovudine (AZT), lamivudine (3TC), nevirapine (NVP), efavirenz (EFV), etravirine (ETV) were selected as the reference drugs. The biological results are expressed as EC₅₀, CC₅₀ and SI (selectivity index, i.e., CC₅₀/EC₅₀ ratio) and summarized in **Table 1** and **Table 2**.

Table 1. Activity and cytotoxicity of **ZL1~21** against HIV-1 (IIB) and HIV-2 (ROD) strains in MT-4 cells.



Comps	R	EC ₅₀ (μM) ^a		CC ₅₀ (μM) ^b	SI ^c	
		IIB	ROD		IIB	ROD
ZL1		0.065±0.023	>33.17	33.17±7.94	511	<1
ZL2		0.020±0.010	137.41±2.36	>241.52	>11830	>2
ZL3		0.013±0.0038	>241.52	>241.52	>18473	X1
ZL4		0.072±0.024	>4.78	4.78±1.84	66	<1
ZL5		0.064±0.015	>128.07	128.07±56.91	1998	<1
ZL6		0.076±0.013	>7.17	7.18±1.59	94	<1
ZL7		0.014±0.0054	>2.10	2.10±0.50	147	<1
ZL8		0.049±0.047	>13.84	13.84±8.55	284	<1

ZL9		0.029±0.015	>81.64	81.64±71.65	3004	<1
ZL10		0.048±0.018	>7.22	7.22±1.21	150	<1
ZL11		0.075±0.038	>101.03	≥101.03	≥1343	<orX1
ZL12		0.045±0.018	>159.69	159.69±43.27	3514	<1
ZL13		0.049±0.022	>8.55	8.55±1.43	175	<1
ZL14		0.16±0.051	>5.69	5.69±0.48	36	<1
ZL15		0.135±0.070	>5.53	5.53±0.23	41	<1
ZL16		0.056±0.014	>6.36	6.36±1.69	113	<1
ZL17		5.62±0.35	>19.78	19.78±20.19	4	<1
ZL18		1.66±0.032	>1.41	1.41±1.27	1	<1
ZL19		2.32±0.34	>10.35	10.35±2.78	4	<1
ZL20		0.27±0.12	>23.76	23.76±8.71	87	<1

ZL21		0.18±0.066	>20.15	20.15±9.59	112	<1
AZT	-	0.012±0.002	0.013±0.002	>7.48	>604	-
3TC	-	7.20±4.13	22.03±3.46	>87.24	>12	-
NVP	-	0.118±0.067	>15.02	>15.02	>51	-
EFV	-	0.003±0.002	>6.34	>6.34	>1205	-
ETV	-	0.003	>4.59	>4.59	>913	-

^aEC₅₀: concentration of compound required to achieve 50% protection of MT-4 cell cultures against HIV-1-induced cytotoxicity, as determined by the MTT method.

^bCC₅₀: concentration required to reduce the viability of mock-infected cell cultures by 50%, as determined by the MTT method.

^cSI: selectivity index, the ratio of CC₅₀/EC₅₀.

As shown in **Table 1**, the biological results clearly showed that most of the newly synthesized compounds exhibited anti-HIV-1 activity from nanomolar to sub-micromolar ranges. Notably, compounds **ZL2**, **ZL3** and **ZL7** turned out to be the most potent HIV-1 inhibitors with the EC₅₀ value of 20 nM, 13 nM and 14 nM against WT HIV-1 strain, which were superior to those reference drugs NVP (EC₅₀ = 0.118 μM), 3TC (EC₅₀ = 7.2 μM) and comparable to AZT (EC₅₀ = 0.012 μM). Besides, all other compounds exhibited considerable potency against the WT strain with EC₅₀ values in the range of 0.029 μM-5.62 μM, which were superior to 3TC. In addition, most of the synthesized compounds displayed decreased cytotoxicity compared with EFV and ETV. Particularly, the two most active compounds exhibit minimal cytotoxicity (**ZL2** and **ZL3**, both CC₅₀ > 241.52 μM) and high selectivity index values (SI > 11830, SI > 18473, respectively).

For the initial exploration, the phenyl group was regarded as the rational hydrophobic group for the purpose of extending to the left hydrophobic channel of the NNIBP, and three compounds **ZL1** - **ZL3** with different substituted phenyl moieties were designed. As expected, all of the three compounds displayed potent anti-HIV-1 activity at nanomolar scale. The preliminary SARs of these novel NNRTIs indicated

that the substituents in the triazole ring have great influence on the anti-HIV activity. For instance, three compounds (**ZL1**, **ZL2**, **ZL3**) with benzene ring directly connected to the triazole showed better inhibitory activity, to be specific, 4-methyl benzoate derivative (**ZL3**) is slightly better than 3-methyl benzoate derivative (**ZL2**), both of them are better than 4-benzoic acid derivative (**ZL1**, $EC_{50}=65$ nM).

To evaluate our hypothesis concerning that some flexible linker between the phenyl and the triazole ring may disturb the rigid structure of phenyl-triazole, and will benefit the “induce-fit” mechanism in the binding of small-molecular inhibitor and NNIBP, compounds **ZL4-ZL13** with the benzyl moiety were designed, synthesized and evaluated for anti-HIV-1 potency. In addition, **ZL4-ZL12** with substituted benzyl groups showed similar potency to the unsubstituted benzyl derivative **ZL13** ($EC_{50}=49$ nM) against WT HIV-1, with the exception of 4-hydroxyl derivative **ZL7** ($EC_{50}=14$ nM) and 4-methanesulfonamide derivative **ZL9** ($EC_{50}=29$ nM), indicating that the hydrogen-bonding donors/acceptor groups have their advantages in potency.

The position of the substituents in the phenyl ring has some influence on the anti-HIV activity. For instance, introduction of a methyl formate group at the C_3 position yielded a 72 nM inhibitor **ZL4**, while the methyl formate group at C_4 position increased the potency to 64 nM. It also indicated that the C_2 or C_4 positions was more favorable for nitril group than C_3 , as **ZL10** (2-nitril, $EC_{50} = 48$ nM) and **ZL12** (4-nitril, $EC_{50} = 45$ nM) were more potent than **ZL11** (3-nitril, $EC_{50} = 75$ nM).

Moreover, the potency is strongly dependent on the nature of the substituents in the phenyl ring. The activity of compounds with the *para*-substitution at the phenyl ring suggested that some polar groups with suitable polarities and electronic nature at the C_4 position might enhance anti-HIV activity by inserting into the hydrophobic channel of NNIBP and making more interactions with the protein-solvent interface. For instance, the hydroxyl-substituted compound **ZL7** ($EC_{50} = 14$ nM) was more potent than the methylformate-substituted compound **ZL6** ($EC_{50} = 76$ nM). However, some substituent groups at C_3 position might show slight influence on the potency. For instance, the 3-methyl formate derivative **ZL4** ($EC_{50} = 72$ nM) displayed similar potency to the 3-nitril derivative **ZL11** ($EC_{50}=75$ nM).

The activity was also influenced by the length and structure of the connecting chain between the aryl moiety and the triazole ring, for example, introduction of a benzyl at the N₄- position yielded a 49 nM inhibitor **ZL13**, while ethylbenzene at this position reduced the potency to 0.16 μM (**ZL14**). Subsequently, the flexible-chain was replaced by a rigid skeleton chain to explore the plasticity of the hydrophobic channel, resulting in three derivatives with the acetylamino linker between the benzene ring and the triazole ring. The substituent groups at C₄ position have great influence on the activity and the order of activity of the *para*-substitution at the phenyl ring was as follows: -SO₂CH₃ (**ZL16**, EC₅₀ = 56 nM) > -F (**ZL18**, EC₅₀ = 1.66 μM) > -Br (**ZL17**, EC₅₀ = 5.62 μM), indicating that this position is preferred over groups with polar groups such as methyl sulfonate and fluorine *et al.*

In addition to the phenyl and substituted phenyl derivatives, other hydrophobic groups were also considered, the thienyl derivative **ZL15** (EC₅₀ = 0.135 μM) showed slight enhanced activity compared to its phenyl analogue **ZL14** (EC₅₀ = 0.16 μM). Moreover, the potency was reduced when the phenyl substituent connecting to the triazole moiety was replaced by the methyl formate moiety. For instance, compound **ZL19** (EC₅₀ = 2.32 μM) and **ZL20** (EC₅₀ = 0.27 μM) showed about 47- and 1.7-fold less potent than the corresponding phenyl derivatives. Moreover, the activity was greatly influenced by the length of the connecting chain between the methyl formate moiety and the triazole ring, the potency was increased when the linker lengths are longer in a suitable range (1-3 atoms were explored in this paper). In particular, the ethyl-linker derivative **ZL20** and the propyl-linker derivative **ZL21** (EC₅₀ = 0.18 μM) were 8.6-fold and 12.9-fold more potent than the methylene-linker derivative **ZL19**.

Furthermore, it is noteworthy that most compounds except **ZL7** and **ZL18** showed extremely low cytotoxicity compared to reference drug ETV. The cytotoxicity is also strongly dependent on the nature of the substituents attached to the triazole. For instance, **ZL2** and **ZL3** with -COOCH₃ substitution at C₃ and C₄ positions in the phenyl ring showed no cytotoxicity (CC₅₀) up to the maximum tested concentration of 241 μM, while addition of a -COOH group to phenyl ring sharply increased the cytotoxicity to 33.17 μM (>7.3-fold). The cytotoxicity of substituted

benzyl derivatives (**ZL4-ZL13**) show significant change ranging from 2.10 μM -159.69 μM . Besides, only compound **ZL2** (EC_{50} = 137.41 μM) showed faint cellular activity against HIV-2 (ROD) in MT-4 cells

View Article Online
DOI: 10.1039/C9OB00032A

Table 2. Activity of **ZL1~21** against HIV-1 mutant strains.

Compds	EC_{50} (μM) ^a						
	L100I	K103N	Y181C	Y188L	E138K	F227L+V106A	RES056
ZL1	0.77±0.018	0.23±0.10	0.84±0.13	6.22±0.19	0.43±0.045	2.73±0.76	3.27±0.069
ZL2	0.47±0.094	0.043±0.019	0.46±0.028	>241.52	0.10±0.01	≥180.4.3	45.24±37.08
ZL3	1.04±0.69	0.022±0.003	0.34±0.055	>241.52	0.16±0.017	>241.52	>241.52
ZL4	>4.78	0.36±0.036	>4.78	>4.78	0.96±0.12	≥2.267	>4.78
ZL5	1.86±0.11	0.35±0.0054	2.11±0.48	≥9.09	0.61±0.0044	≥9.22	≥37.66
ZL6	>7.18	0.42±0.094	>7.18	>7.18	0.56±0.14	>7.18	>7.18
ZL7	≥0.35	0.054±0.009	0.53±0.40	>2.10	0.091±0.010	>2.10	>2.10
ZL8	0.63±0.11	0.068±0.028	0.56±0.032	1.33±0.13	0.12±0.021	>13.84	>13.84
ZL9	0.61±0.090	0.10±0.0005	0.53±0.020	≥3.56	0.12±0.0028	>86.44	>86.44
ZL10	>7.22	0.31±0.022	>7.22	>7.22	0.50±0.11	>7.22	>7.22
ZL11	9.45±7.02	0.38±0.050	4.44±0.22	4.54±0.43	0.51±0.010	>101.03	>101.03
ZL12	1.52±0.19	0.17±0.0054	1.42±0.97	≥36.49	0.33±0.0095	33.83±0.98	>159.69
ZL13	1.11±0.10	0.22±0.057	1.42±0.39	>8.55	0.24±0.098	>8.55	>8.55
ZL14	>5.66	0.42±0.012	>5.66	>5.66	≥2.05	>5.66	>5.66
ZL15	>5.53	0.37±0.018	>5.53	>5.53	0.61±0.059	>5.53	>5.53
ZL16	>6.36	1.04±0.12	>6.36	>6.36	1.23±0.099	>6.36	>6.36
ZL17	>19.78	>19.78	>19.78	>19.78	>19.78	>19.78	>19.78
ZL18	>1.41	>1.41	>1.41	>1.41	>1.41	>1.41	>1.41
ZL19	>10.35	6.64±1.43	>10.35	>10.35	>10.35	>10.35	>10.35
ZL20	5.06±0.43	0.75±0.0096	3.37±0.23	>23.76	1.03±0.048	>23.76	>23.76
ZL21	7.10±0.49	0.79±0.26	≥7.16	>20.15	1.68±0.24	>20.15	>20.15
AZT	0.006±0.001	0.019±0.013	0.008±0.001	0.007±0.001	0.016±0.005	0.007±0.002	0.02±0.007
3TC	2.46±0.30	3.76±1.23	4.40±1.60	4.06±0.75	5.54±1.86	2.74±0.78	5.56±0.70
NVP	2.22±1.31	12.35±0.88	>15.02	>15.02	0.18±0.039	>15.02	>15.02
EFV	0.046±0.009	0.11±0.035	0.006±0.001	0.307±0.054	0.005±0.001	0.269±0.049	0.265±0.048
ETV	0.006±0.002	0.003±0.0004	0.012±0.003	0.017±0.006	0.008±0.003	0.014±0.005	0.043±0.015

^a EC_{50} : concentration of compound required to achieve 50% protection of MT-4 cell cultures against HIV-1-induced cytotoxicity, as determined by the MTT method.

Table 3. Resistance folds for the K103N mutant strain of selected compounds in MT-4 cells.

Compds	Resistance Folds ^a
	K103N
ZL2	2.2
ZL3	1.7
ZL7	3.9
ZL8	1.4
EFV	36.7

^aResistance Fold: RF, ratio of EC₅₀ against mutant strain/EC₅₀ against WT strain.

The activity of the newly synthesized compounds was further evaluated against a panel of clinical relevant HIV-1 mutant strains, including L100I, K103N, Y181C, Y188L, E138K, F227L+V106A, and RES056, in MT-4 cells. In the case of the mutant HIV-1 strains (**Table 2**), most compounds displayed potent activity against single mutant HIV-1 strains, especially to K103N and E138K. As for K103N, which is the most common mutation emerging in HIV patients treated with EFV, five compounds provided double-digit nanomolar activity. In particular, **ZL3** (EC₅₀ = 0.022 μM) was notably more active than 3TC, NVP and EFV and compared to AZT. Regarding the resistance fold (**Table 3**), compounds **ZL2**, **ZL3**, **ZL7**, **ZL8** showed no significant decrease in activity (RF = 2-6) for K103N while EFV had the RF of 36.7. Furthermore, compounds **ZL1**, **ZL2**, **ZL8** and **ZL9** showed higher activity towards mutant HIV-1 strain L100I (EC₅₀ = 0.77, 0.47, 0.63, 0.61 and 0.57 μM, respectively), being far more potent than 3TC (EC₅₀ = 2.46 μM) or NVP (EC₅₀ = 2.22 μM). Other seven compounds (**ZL3**, **ZL5**, **ZL11-13**, **ZL20-21**) showed moderate activity. However, the remaining nine compounds lacked activity towards this mutant strain. Intriguingly, except for **ZL17** and **ZL18**, all the target compounds displayed good activity against K103N with EC₅₀ values in the range of 0.022-10.85 μM. Furthermore, **ZL3** and **ZL8** respectively showed the most potent activity against the single mutants Y181C and Y188L with EC₅₀ = 0.34 μM and 0.675 μM. Interestingly, all the target compounds displayed good activity against E138K with EC₅₀ values in the range of 0.091-1.68 μM, and the inhibitory activity of most compounds is at the submicromolar level. Moreover, **ZL1** and **ZL12** were effective inhibitors of the double-mutant strain F227L+V106A with EC₅₀ values of 2.73 and 33.83 μM, respectively. **ZL1** also show the best inhibitory activity towards RES056 with EC₅₀ of

3.27 μM . However, the other compounds were inactive towards these double mutant strains except **ZL2** ($\text{EC}_{50} = 45.24 \mu\text{M}$).

View Article Online
DOI: 10.1039/C9OB00032A

2.3. Inhibition of HIV-1 RT

To validate the binding target of these novel NNRTIs, all compounds were further tested for their ability to inhibit recombinant WT HIV-1 RT enzymes; the results are shown in **Table 3**. In the enzymatic assay, all the tested compounds exhibited potent inhibitory activities toward WT HIV-1 RT with IC_{50} values ranging from 0.02 μM to 0.76 μM .

Table 4. Inhibitory activity of compounds against HIV-1 WT RT

Compds	IC_{50} (μM) ^a
ZL1	0.02
ZL2	0.05
ZL3	0.06
ZL4	0.22±0.01
ZL5	0.24±0.04
ZL6	0.40±0.12
ZL7	0.04±0.01
ZL8	0.06±0.02
ZL9	0.11±0.06
ZL10	0.15±0.01
ZL11	0.24±0.04
ZL12	0.15±0.02
ZL13	0.18
ZL14	0.62±0.07
ZL15	0.44±0.11
ZL16	0.29±0.05
ZL17	0.76±0.10
ZL18	0.36±0.03
ZL19	0.39±0.05
ZL20	0.14±0.01
ZL21	0.21±0.04
NVP	0.49±0.26
EFV	0.007±0.002
ETV	1.35±0.35

^a IC_{50} : Inhibitory concentration of test compound required to inhibit biotin deoxyuridine triphosphate (biotin-dUTP) incorporation into HIV-1 WT RT by 50%.

The result showed that all compounds exhibited potent activity toward WT RT with IC_{50} values ranging from 0.02 to 0.76 μM , and most of the compounds were superior to NVP ($IC_{50} = 0.49 \mu\text{M}$) and ETV ($IC_{50} = 1.35 \mu\text{M}$) (**Table 4**). The three most potent compounds **ZL1**, **ZL2** and **ZL7** exhibited higher enzymatic inhibition activity ($IC_{50} = 0.02, 0.05$ and $0.04 \mu\text{M}$, respectively). Among them, 4-benzoic acid derivative **ZL1** displayed the most potent activity toward WT RT, indicating carboxylic acid moiety has better enzyme inhibitory activity and this phenomenon has been identified in our previous research. However, the markedly decreased potency against WT HIV-1 of **ZL1** in cell culture may be due to its negative charged form under experimental conditions influencing its cell membrane permeability. On the whole, all these novel derivatives are RT and they all acted as classical NNRTIs.

It is noteworthy that the antiviral activity of some compounds in this study was inconsistent with its enzyme-inhibitory potency to some extent. These differences may be explained by template-specific variation in the relationship between HIV-RT-RNA binding affinity and polymerase processivity, which has been observed in most NNRTI series.²⁷ Besides, there is a high probability of formation of cocrystals or salts due to the multiple hydrogen bond donor and acceptor sites in these compounds.

2.4. Molecular modeling analysis

In order to obtain further insight into the allosteric binding of 1,2,3-triazole-derived diarylpyrimidines to the NNIBP of RT, by means of software SYBYL-X 2.0, the most potent three compounds **ZL2**, **ZL3** and **ZL7** in the enzymatic assay was conducted further docking studies utilizing the structures of cocrystal of WT RT (PDB code: 2ZD1 and 3MEG). Our docking results were visualized by PyMOL. And the docking protocol was illustrated in the computational section.

The docking simulations of these molecules with HIV-1 WT RT revealed that the binding mode resembles those classical NNRTI drugs (**Figures 4**): the left wing of these compounds occupies the hydrophobic channel formed by aromatic amino acid residues Y181, Y188, F227, and W229, exhibiting π - π interaction with these residues

and the substituent group in the triazole ring further stretch into protein-solvent interface and can develop extensive interactions with surrounding residues or water molecule, thereby improving the stability of the RT-inhibitor complex; Of particular note is that both **ZL3** and **ZL7** form “water bridge” hydrogen bonds with L228, which explain the excellent anti-HIV-1 activity. Besides, the pyrimidine heterocycle and the NH linker connecting the central pyridine ring maintained the “signature” double hydrogen bonds with the backbone of K101; The right 4-cyanoaniline was located in another pocket and interacted with residues V106, L234, P236 and Y318.

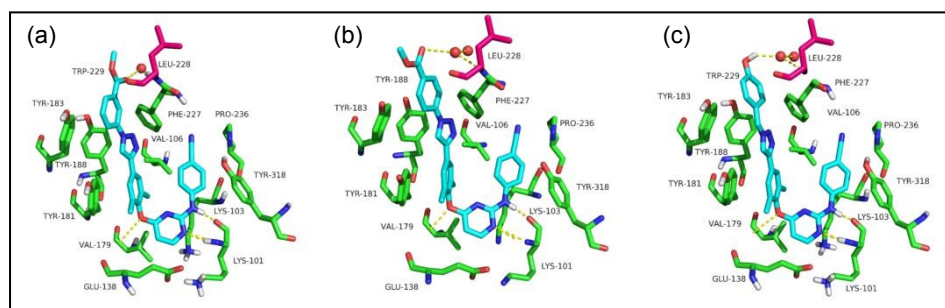
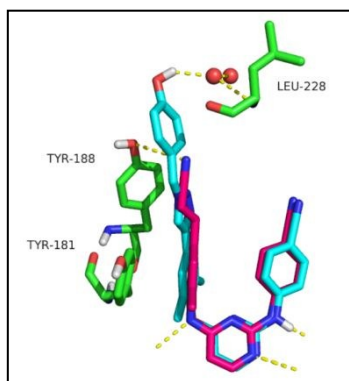


Figure 4. Predicted binding modes of **ZL2**, **ZL3** and **ZL7** with the crystal structures of HIV-1 WT RT (PDB: 2ZD1). The hydrogen bonds between the inhibitors and amino acid residues are indicated with dashed lines (yellow). Ligand carbon atoms are shown in cyan, and protein carbon atoms in green and magenta. The water molecules are shown in red ball. Nonpolar hydrogen atoms are hid for clarity.

Although these compounds are still able to maintain a good U-shaped conformation, the activity is reduced compared to the lead compounds. From the superposition of compound **ZL7** and RPV in molecular docking (**Figure 5**), the left benzene ring of **ZL7** was shift away from the benzene ring of RPV despite of the well-superimposition in right wing, causing the disappearance of π - π interaction between the left benzene ring and Y181. Further, **ZL7** develops water-mediated hydrogen bonds with L228 instead of the hydrogen bond connecting hydroxyl- and cyano group on RPV, compensating for the decline in compounds inhibitory activity to some extent.



View Article Online
DOI: 10.1039/C9OB00032A

Figure 5. Superimposition of **ZL7** (cyan) and **RPV** (hot pink) with HIV-1 WT RT (PDB: 2ZD1). The hydrogen bonds between the inhibitors and amino acid residues are indicated with dashed lines (yellow). Ligand carbon atoms are shown in cyan, and protein carbon atoms in green. The water molecules are shown in red ball. Nonpolar hydrogen atoms are hid for clarity.

When docking into the K103N mutant RT, **ZL2** and **ZL3** cannot enter the binding pocket of RT by the original mode (**Figure 6a, 6b**), causing the decreased activity. However, the distorted structure stretches into the entrance channel and formed new hydrogen bond with N103, compensating the affinity loss with sub-pocket in NNIBP to some extent, and this may be the reason why **ZL2** and **ZL3** possessed the most potent activity against K103N mutant HIV-1 strain. Regarding to the binding mode of **ZL7** in the NNIBP, it still maintained a hydrogen bond with K101 and furthermore formed new hydrogen bond with Y186. As we all know, Y186 plays an important role in the catalytic active site of RT, this directed us to modify targeting the active site next step.

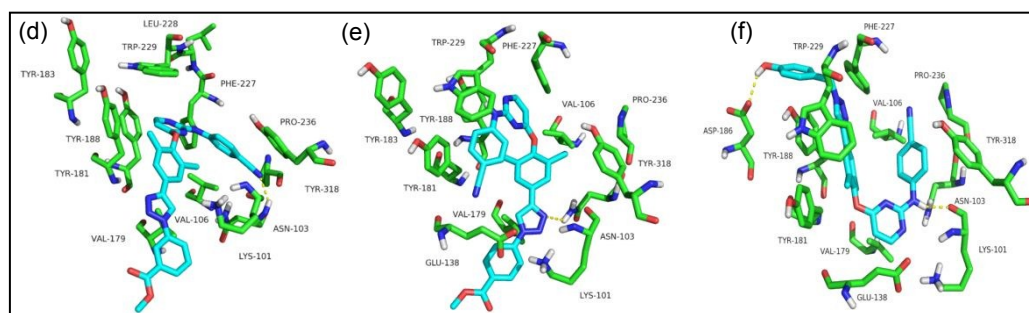


Figure 6. Predicted binding modes of **ZL2**, **ZL3** and **ZL7** with the crystal structures of HIV-1 K103N RT (PDB: 3MEG). The hydrogen bonds between the inhibitors and amino acid residues are indicated with dashed lines (yellow). Ligand carbon atoms are shown in cyan, and protein carbon atoms in green. Nonpolar hydrogen atoms are hidden for clarity.

2.5. Water solubility and other drug-like properties

View Article Online
DOI: 10.1039/C9OB00032A

Aqueous solubility of the compounds was the important physicochemical property which could make a huge impact on the biological evaluation. So the water solubility of the representative compounds **ZL2**, **ZL3** and **ZL7** were tested. As revealed in Table 5, all three compounds possessed significantly improved water solubility than that of ETV at different pH values, which may due to the good water solubility of 1,2,3-triazole moiety. Furthermore, the preliminary physicochemical properties of representative compounds **ZL2**, **ZL3** and **ZL7** were examined to evaluate their drug-like properties by utilizing free online molinspiration software (<http://www.molinspiration.com/>). Lipophilic parameter ligand efficiency (LE) was also calculated. The results (**Table 5**) suggested that parameters like molecular weight (MW), hydrogen bond acceptors (nON), molinspiration predicted LogP (miLogp), and ligand efficiency (LE) for **ZL2** and **ZL3** were inconsistent with the Lipinski's rule of five. In addition, **ZL7** showed the slightest deviation for miLogp and LE for all tested compounds. Therefore, it is supposed that **ZL7** may have the acceptable physicochemical properties. Besides, the topological polar surface area (tPSA), which is characterized by the absorption and membrane permeability of molecules, showed the three compounds had a value ranging from 121.78 to 127.86 Å², confirming their advantage for intestinal absorption (<140 Å²) and inability to penetrate the blood-brain barrier, averting the central nervous system toxicity (>60 Å²).

Table 5. Water solubility and physicochemical properties of representative compounds and ETV.

Parameter items ^a	ZL2	ZL3	ZL7	ETV
Water solubility (pH=2, µg/ml)	18.2±0.09	25.0±0.08	23.0±0.30	
Water solubility (pH=7, µg/ml)	36.5±0.31	36.3±0.17	38.7±0.13	<<1
Water solubility (pH=7.4, µg/ml)	30.8±0.15	43.3±0.11	30.8±0.10	
natoms	39	39	36	28
MW (< 500 Da)	517.55	517.55	475.51	435.29
nON (< 10)	10	10	9	7
nOHNH (< 5)	1	1	2	3
Nrotb (<10)	8	8	6	4
tPSA (<140 Å ²)	127.86	127.86	121.78	120.65
MV	454.32	454.32	417.81	335.95

miLog p (< 5)	5.93	5.74	5.09	5.03
nViol	2	2	1	1
LE (>0.3)	0.27	0.28	0.30	0.42

View Article Online
DOI: 10.1039/C9OB00032A

^a nViol = number of violations; natoms = no. of atoms; miLogP = molinspiration predicted LogP; MW = molecular weight; nON = no. of hydrogen bond acceptors; nOHNH = no. of hydrogen bond donors; nrotb = no. of rotatable bonds; TPSA = topological polar surface area; MV = molar volume; LE = calculated by the formula $-\Delta G/HA$ (non-hydrogen atom), in which normalizing binding energy $\Delta G = -2.303RT \log K_d$, presuming $K_d \approx EC_{50}(III B)$; $R = 1.987 \times 10^{-3}$ kcal/K/mol, $T = 298$ K.

2.6 *In Vitro* Effects of ZL3 on CYP Enzymatic Inhibitory Activity

As is well known, metabolizing enzymes in the liver (e.g. cytochrome P450, CYP) are responsible for the majority of drug metabolism *in vivo*. CYP enzymes are considered to be one of the most important enzyme families for drug-drug interaction (DDI) assessments due to the involvement of these enzymes in the metabolic clearance of the majority of prescribed drugs. The evaluation of cytochrome CYP enzyme inhibition/inactivation development remains an important factor in overall risk assessment and compound progression to the clinic. In addition, three main subtypes CYP3A, CYP2D6 and CYP2C are involved in metabolism of about 90% of the marketed drugs. Therefore, metabolism-mediated DDIs may occur when co-administrating different drugs, leading to decreased therapeutic effect or adverse reaction profile. According to reported study, etravirine is an inducer of CYP3A4 and inhibitor of CYP2C9 and CYP2C19, and it can result in many drug-drug interactions when co-administrated with other anti-HIV-1 drugs like protease inhibitors, integrase strand inhibitors and CCR5 antagonists etc, which influence the use of concomitant antiretrovirals. We performed the study of inhibitory activity of compound **ZL3** on main CYP drug metabolizing enzymes, with selective inhibitors of these enzymes as positive controls. The results in **Table 6** indicated that **ZL3** displayed no CYP enzymatic inhibition of CYP1A2, CYP2C19, CYP2D6 and CYP3A4M, however, it exhibits strong inhibitory activity against CY2C9.

Table 6. Inhibitory activity on CYP1A2, CY2C9, CYP2C19, CYP2D6 and CYP3A4M of compound **ZL3** and positive controls

CYP Isozyme	Standard Inhibitor	Inhibitory activity (IC ₅₀ , μM)	Compd	Inhibitory activity (IC ₅₀ , μM)
1A2	α-Naphthoflavone	0.289	ZL3	>50
2C9	Sulfaphenazole	0.585	ZL3	0.113
2C19	(+)-N-3-benzylrivanol	0.179	ZL3	>50
2D6	Quinidine	0.136	ZL3	>50
3A4	Ketoconazole	0.0423	ZL3	>50

View Article Online
DOI: 10.1039/C9OB00032A

3. Conclusion

In general, a series of novel triazole derivatives targeting the hydrophobic channel of NNIBP were rationally designed based on structure-guided approach, synthesized and evaluated for their inhibitory activity against HIV-1 (including IIB, L100I, K103N, E138K, Y181C, Y188L, F227L+V106A, K103N+Y181C and HIV-2 (ROD) strains) in MT-4 cells. All compounds showed excellent to good activity against wild-type HIV-1 strain with EC₅₀ ranging from 0.013 μM to 5.97 μM. It is noteworthy that, regarding the inhibitory activity against K103N, the major drug resistant mutant to the new generation HIV-1 NNRTIs, three promising compounds **ZL2**, **ZL3**, and **ZL7** are superior to the first-line antiretroviral drugs efavirenz. More encouragingly, **ZL2** and **ZL3** exhibited much lower cytotoxicity and high selection index of >10,000 compared with all the reference drugs (AZT, 3TC, NVP, EFV, ETV). In addition, the inhibition of HIV RT indicated that most of these compounds could effectively inhibit the activity of HIV-1 RT at low micromolar concentrations, confirming their target is HIV-1 RT. Furthermore, detailed SAR and docking study of the representative compounds help us to understand the binding modes of the compounds in the NNIBP and guide future optimization, which is ongoing in our lab aimed at improving drug resistance profiles and reducing the cytotoxicity and will be reported in due course. Subsequently, the preliminary physicochemical properties and the early metabolic stability of representative compounds were examined to evaluate their drug-like properties. Three tested compounds **ZL2**, **ZL3** and **ZL7** showed significantly improved water solubility than that of ETV. In the CYP enzymatic inhibitory assay, **ZL3** displayed no CYP enzymatic inhibition of CYP1A2, CYP2C19,

CYP2D6 and CYP3A4M but strong inhibitory activity against CY2C9, which should be considered in further drug development.

To sum up, the biological activity and docking studies indicated that the hydrophobic channel of NNIBP can accommodate various substituents and are worth further exploring. In addition, it is essential to choose the appropriate linker moiety and try to make the substituent groups structurally diverse to explore the left hydrophobic channel.

4. Experimental section

4.1. Chemistry

^1H NMR and ^{13}C NMR spectra were recorded on a Bruker AV-400 spectrometer using solvents as indicated ($\text{DMSO-}d_6$). Chemical shifts were reported in δ values (ppm) with tetramethylsilane as the internal reference, and J values were reported in hertz (Hz). Mass spectra were performed on a LC Autosampler Device: Standard G1313A instrument. Melting points (m.p.) were determined on a micromelting point apparatus (Tian Jin Analytical Instrument Factory, Nankai, Tianjin, China). TLC was performed on Silica Gel GF254 for TLC (Merck) and spots were visualized by irradiation with UV light ($\lambda=254$ nm). Flash column chromatography was performed on column packed with Silica Gel60 (200-300 mesh). Thin layer chromatography was performed on pre-coated HUANGHAI_HSGF254, 0.15-0.2 mm TLC-plates. Solvents were of reagent grade and were purified and dried by standard methods when necessary. Concentration of the reaction solutions involved the use of rotary evaporator at reduced pressure.

4.1.1. 4-((6-oxo-1,6-dihydropyrimidin-2-yl)amino)benzotrile (**2**).

2-(Methylthio)pyrimidin-4(3H)-one (**1**) (3 g, 0.021 mol) was reacted with 4-aminobenzotrile (2.99 g, 0.025 mol) at 180°C by melting method for 8h. After cooling, CH_3CN (20 mL) was added to dissolve the mixture by ultrasound treatment. Thereafter, the reaction mixture was filtered and washed with CH_3CN until no residual 4-aminobenzotrile was detected by TLC. It was then dried in vacuo to give the product 4-((4-oxo-1,4-dihydropyrimidin-2-yl)amino)benzotrile (**2**) as a light yellow solid, yield 73.6%, ESI-MS: m/z 213.3 $[\text{M}+\text{H}]^+$, $\text{C}_{11}\text{H}_8\text{N}_4\text{O}$ (212.12).

4.1.2. 4-((4-chloropyrimidin-2-yl)amino)benzonitrile (**3**).

View Article Online
DOI: 10.1039/C9OB00032A

A mixture of 4-((4-oxo-1,4-dihydropyrimidin-2-yl)amino)benzonitrile (**2**) (0.80 g, 0.0038 mol) in POCl₃ (5 mL) was refluxed for 0.5 h. Then, the mixture was slowly poured into icy water (50 mL) vigorously stirring. Subsequently, the mixture was filtered to give a filtrate cake, which was then again added into water (10 mL) and was neutralized to pH = 7 with sodium hydroxide. The product was obtained by filtration and dried under vacuo to provide 4-((4-chloropyrimidin-2-yl)amino)benzonitrile (**3**) as pale yellow solids with the yield of 71.3%; ¹H NMR (400 MHz, DMSO-*d*₆) δ 10.58 (s, 1H), 8.55 (d, *J* = 5.2 Hz, 1H, C₆-pyrimidine-H), 7.87 (dd, 4H, Ph-H), 7.13 (d, *J* = 5.2 Hz, 1H, C₆-pyrimidine-H); ESI-MS: *m/z* 231.2 [M+H]⁺, C₁₁H₇ClN₄ (230.04).

4.1.3. 4-((4-(4-iodo-2,6-dimethylphenoxy)pyrimidin-2-yl)amino)benzonitrile (**4**).

In a schlenk-type flask, intermediates **3** (1.0 equiv), 4-((4-(4-iodo-2,6-dimethylphenoxy)pyrimidin-2-yl)amino)benzonitrile (1.0 equiv) and K₂CO₃ (1.2 equiv) were dissolved in DMF stirring for 10h at 100°C. The solution was cooled to room temperature, and water was added to it. The resulting precipitate was purified on silica gel gave intermediates **4**.

4.1.4. 4-((4-(2,6-dimethyl-4-((trimethylsilyl)ethynyl)phenoxy)pyrimidin-2-yl)amino)benzonitrile (**5**)

Trimethylsilylacetylene (3.0 equiv) was added to a solution of intermediates **4** (1.0 equiv), cuprous iodide (0.10 equiv), bis(triphenylphosphine) palladium(II) dichloride (0.05 equiv) and trimethylamine (3 equiv) in anhydrous THF. The mixture was stirred at room temperature under nitrogen atmosphere and monitored by TLC until its completion. After cooling, the solvent was filtered using diatomaceous earth and then evaporated. The residue was purified by flash column chromatography using ethyl acetate/petroleum ether as eluent to obtain intermediate **5**.

4.1.4. 4-((4-(4-ethynyl-2,6-dimethylphenoxy)pyrimidin-2-yl)amino)benzonitrile (**6**)

In a schlenk-type flask, **5** (1.0 equiv) and NaOH (1.2 equiv) were dissolved in methanol stirring for 10h at room temperature. Purification on silica gel gave the important intermediate **6**.

4.1.5. General procedure for synthesis of target compounds (**ZL1-ZL21**).

The key intermediate **6** (1.0 eq), azide substituents (1.1 eq), ascorbic acid sodium (0.6 eq) and $\text{CuSO}_4 \cdot 5\text{H}_2\text{O}$ (0.3 eq) were dissolved in the solution of tetrahydrofuran/water (V:V= 1:1). The resulting mixture was stirred at rt for 4-6 h. Then the reaction mixture was extracted with ethyl acetate (3×10 mL), and the combined organic phase was washed with saturated salt water (3×10 mL), dried over anhydrous NaSO_4 , filtered, and concentrated under reduced pressure to give the corresponding crude target product, which was purified by flash column chromatography to afford product **ZL1-21**.

*4-(4-(4-((2-((4-cyanophenyl)amino)pyrimidin-4-yl)oxy)-3,5-dimethylphenyl)-1H-1,2,3-triazol-1-yl)benzoic acid (**ZL1**).*

Recrystallized from EA/PE as a white solid, 57.3% yield, m.p. 303 – 306 °C; ^1H NMR (400 MHz, $\text{DMSO}-d_6$) δ 13.18 (s, 1H, COOH), 10.08 (s, 1H, NH), 9.41 (s, 1H, triazole-H), 8.42 (d, $J = 5.7$ Hz, 1H, C_6 -pyrimidine-H), 8.25 – 7.99 (m, 4H, Ph-H), 7.75 (s, 2H, Ph-H), 7.59 (d, $J = 8.4$ Hz, 2H, Ph-H), 7.39 (d, $J = 8.4$ Hz, 2H, Ph-H), 6.60 (d, $J = 5.7$ Hz, 1H, C_5 -pyrimidine-H), 2.10 (s, 6H, 2CH_3). ^{13}C NMR (100 MHz, $\text{DMSO}-d_6$) δ 168.96, 166.91, 160.79, 159.69, 149.95, 147.67, 145.07, 139.97, 133.06, 131.66, 131.64, 128.08, 126.40, 120.07, 119.83, 118.73, 102.92, 99.43, 16.69; ESI-MS: m/z 504.4 $[\text{M}+\text{H}]^+$. $\text{C}_{28}\text{H}_{21}\text{N}_7\text{O}_3$ (503.17).

*Methyl 3-(4-(4-((2-((4-cyanophenyl)amino)pyrimidin-4-yl)oxy)-3,5-dimethylphenyl)-1H-1,2,3-triazol-1-yl)benzoate (**ZL2**).*

Recrystallized from EA/PE as a white solid, 62.4% yield, m.p.: 232-234°C; ^1H NMR (400 MHz, $\text{DMSO}-d_6$) δ 10.17 (s, 1H, NH), 9.53 (s, 1H, triazole-H), 8.56 – 8.47 (m, 2H, Ph-H, C_6 -pyrimidine-H), 8.31 (dd, $J = 7.9, 2.2$ Hz, 1H, Ph-H), 8.09 (d, $J = 7.8$ Hz, 1H, Ph-H), 7.83 (d, $J = 6.8$ Hz, 3H, Ph-H), 7.67 (d, $J = 8.4$ Hz, 2H, Ph-H), 7.47 (d, $J = 8.5$ Hz, 2H, Ph-H), 6.67 (d, $J = 5.6$ Hz, 1H, C_5 -pyrimidine-H), 3.95 (s, 3H, CH_3), 2.18 (s, 6H, 2CH_3). ^{13}C NMR (100 MHz, $\text{DMSO}-d_6$) δ 168.97, 165.77, 160.77, 159.69, 149.89, 147.62, 145.07, 137.35, 133.06, 131.81, 131.61, 131.13, 129.52, 128.15, 126.36, 124.71, 120.41, 119.82, 118.71, 102.90, 99.42, 53.07, 16.69. ESI-MS: m/z 518.4 $[\text{M}+\text{H}]^+$. $\text{C}_{29}\text{H}_{23}\text{N}_7\text{O}_3$ (517.19).

Methyl 4-(4-(4-((2-((4-cyanophenyl)amino)pyrimidin-4-yl)oxy)-3,5-dimethylphenyl)-1H-1,2,3-triazol-1-yl)benzoate (ZL3).

Recrystallized from EA/PE as a white solid, 62.3% yield, m.p. 252 – 254 °C; ¹H NMR (400 MHz, DMSO-*d*₆) δ 10.15 (s, 1H, NH), 9.52 (s, 1H, triazole-H), 8.53 (t, *J* = 1.9 Hz, 1H, Ph-H), 8.49 (d, *J* = 5.6 Hz, 1H, C₆-pyrimidine-H), 8.30 (d, *J* = 7.9, 2.3 Hz, 1H, Ph-H), 8.09 (d, 1H, Ph-H), 7.87 – 7.78 (m, 3H, Ph-H), 7.68 (d, *J* = 8.5 Hz, 2H, Ph-H), 7.47 (d, *J* = 8.5 Hz, 2H, Ph-H), 6.67 (d, *J* = 5.6 Hz, 1H, C₅-pyrimidine-H), 3.95 (s, 3H, CH₃), 2.18 (s, 6H, 2CH₃). ¹³C NMR (100 MHz, DMSO-*d*₆) δ 168.98, 165.77, 160.77, 159.69, 149.89, 147.62, 145.07, 137.35, 133.05, 131.82, 131.60, 131.12, 129.52, 128.16, 126.37, 124.71, 120.43, 119.81, 118.73, 102.92, 99.42, 53.06, 16.68. ESI-MS: *m/z* 518.4 [M+H]⁺. C₂₉H₂₃N₇O₃ (517.19).

Methyl 3-((4-(4-((2-((4-cyanophenyl)amino)pyrimidin-4-yl)oxy)-3,5-dimethylphenyl)-1H-1,2,3-triazol-1-yl)methyl)benzoate (ZL4).

Recrystallized from EA/PE as a white solid, 71.8% yield, m.p. 197 – 198 °C; ¹H NMR (400 MHz, DMSO-*d*₆) δ 10.05 (s, 1H, NH), 8.61 (s, 1H, triazole-H), 8.39 (d, *J* = 5.6 Hz, 1H, C₆-pyrimidine-H), 7.94 – 7.84 (m, 2H, Ph-H), 7.64 (s, 2H, Ph-H), 7.61 – 7.46 (m, 4H, Ph-H), 7.36 (d, *J* = 8.4 Hz, 2H, Ph-H), 6.56 (d, *J* = 5.6 Hz, 1H, C₅-pyrimidine-H), 5.72 (s, 2H, CH₂), 3.79 (s, 3H, CH₃), 2.05 (s, 6H, 2CH₃). ¹³C NMR (100 MHz, DMSO-*d*₆) δ 168.99, 166.32, 160.75, 159.67, 149.59, 146.82, 145.07, 137.21, 133.22, 133.03, 131.45, 130.62, 129.90, 129.42, 129.07, 128.64, 126.18, 122.07, 119.80, 118.69, 102.88, 99.37, 53.02, 52.73, 16.60. ESI-MS: *m/z* 532.4 [M+H]⁺. C₃₀H₂₅N₇O₃ (531.20).

Methyl 4-((4-(4-((2-((4-cyanophenyl)amino)pyrimidin-4-yl)oxy)-3,5-dimethylphenyl)-1H-1,2,3-triazol-1-yl)methyl)benzoate (ZL5).

Recrystallized from EA/PE as a light yellow solid, 69.7% yield, m.p. 221 – 223 °C; ¹H NMR (400 MHz, DMSO-*d*₆) δ 10.15 (s, 1H, NH), 8.69 (s, 1H, triazole-H), 8.47 (d, *J* = 5.6 Hz, 1H, C₆-pyrimidine-H), 8.01 (d, *J* = 8.2 Hz, 2H, Ph-H), 7.72 (s, 2H, Ph-H), 7.62 (d, *J* = 8.5 Hz, 2H, Ph-H), 7.47 (d, *J* = 8.1 Hz, 2H, Ph-H), 7.42 (d, *J* = 8.5 Hz, 2H, Ph-H), 6.64 (d, *J* = 5.6 Hz, 1H, C₅-pyrimidine-H), 5.81 (s, 2H, CH₂), 3.86 (s, 3H, CH₃), 2.12 (s, 6H, 2CH₃). ¹³C NMR (100 MHz, DMSO-*d*₆) δ 168.97, 166.32,

160.80, 159.64, 149.63, 146.82, 145.07, 141.71, 133.02, 131.47, 130.18, 129.82, 128.63, 128.46, 126.18, 122.25, 119.82, 118.68, 102.84, 99.35, 53.06, 52.69, 16.60.
ESI-MS: m/z 532.3 $[M+H]^+$. $C_{30}H_{25}N_7O_3$ (531.20).

4-((4-(4-(1-(4-cyanobenzyl)-1H-1,2,3-triazol-4-yl)-2,6-dimethylphenoxy)pyrimidin-2-yl)amino)benzotrile (ZL6).

Recrystallized from EA/PE as a white solid, 65.3% yield, m.p.: 225-227°C; 1H NMR (400 MHz, DMSO- d_6) δ 10.13 (s, 1H, NH), 8.68 (s, 1H, triazole-H), 8.47 (d, J = 5.6 Hz, 1H, C₆-pyrimidine-H), 7.95 (dd, J = 7.7, 1.3 Hz, 1H, Ph-H), 7.85 – 7.68 (m, 3H, Ph-H), 7.69 – 7.54 (m, 3H, Ph-H), 7.44 (dd, J = 12.1, 8.2 Hz, 3H, Ph-H), 6.64 (d, J = 5.6 Hz, 1H, C₅-pyrimidine-H), 5.91 (s, 2H, CH₂), 2.13 (s, 6H, 2CH₃). ^{13}C NMR (100 MHz, DMSO- d_6) δ 168.98, 160.77, 159.66, 149.64, 146.68, 145.07, 139.19, 134.36, 133.93, 133.03, 131.48, 129.88, 129.72, 128.54, 126.19, 122.49, 119.81, 118.68, 117.40, 111.69, 102.88, 99.38, 51.77, 40.21, 16.60; ESI-MS: m/z 499.4 $[M+H]^+$. $C_{29}H_{22}N_8O$ (498.19).

4-((4-(4-(1-(4-hydroxybenzyl)-1H-1,2,3-triazol-4-yl)-2,6-dimethylphenoxy)pyrimidin-2-yl)amino)benzotrile (ZL7).

Recrystallized from EA/PE as a white solid, 66.4% yield, m.p. 255 – 258 °C; 1H NMR (400 MHz, DMSO- d_6) δ 10.08 (s, 1H, NH), 9.26 (s, 1H, triazole-H), 8.41 (d, J = 5.6 Hz, 1H, C₆-pyrimidine-H), 7.87 (d, J = 8.2 Hz, 2H, Ph-H), 7.74 (s, 2H, Ph-H), 7.59 (d, J = 8.5 Hz, 2H, Ph-H), 7.51 (d, J = 8.2 Hz, 2H, Ph-H), 7.38 (d, J = 8.5 Hz, 2H, Ph-H), 6.59 (d, J = 5.6 Hz, 1H, C₅-pyrimidine-H), 5.32 (t, J = 5.7 Hz, 1H, OH), 4.54 (d, J = 5.7 Hz, 2H, CH₂), 2.10 (s, 6H, 2CH₃). ^{13}C NMR (100 MHz, DMSO- d_6) δ 168.98, 160.79, 159.68, 149.82, 147.34, 145.07, 143.77, 135.73, 133.06, 131.58, 128.37, 128.14, 126.34, 120.16, 119.96, 119.83, 118.72, 102.90, 99.42, 62.70, 16.69. ESI-MS: m/z 490.4 $[M+H]^+$. $C_{28}H_{23}N_7O_2$ (489.19).

4-((4-(4-((2-((4-cyanophenyl)amino)pyrimidin-4-yl)oxy)-3,5-dimethylphenyl)-1H-1,2,3-triazol-1-yl)methyl)benzamide (ZL8).

Recrystallized from EA/PE as a white solid, 75.3% yield, m.p. 289 – 290 °C; 1H NMR (400 MHz, DMSO- d_6) δ 10.13 (s, 1H, NH), 8.67 (s, 1H, triazole-H), 8.47 (d, J = 5.6 Hz, 1H, C₆-pyrimidine-H), 7.98 (s, 1H, Ph-H), 7.90 (d, J = 8.2 Hz, 2H, Ph-H),

7.71 (s, 2H, NH₂), 7.64 (d, $J = 8.5$ Hz, 2H, Ph-H), 7.49 – 7.39 (m, 5H, Ph-H), 6.63 (d, $J = 5.6$ Hz, 1H, C₅-pyrimidine-H), 5.76 (d, $J = 5.3$ Hz, 2H, CH₂), 2.12 (s, 6H, 2CH₃). ¹³C NMR (101 MHz, DMSO) δ 168.99, 167.88, 160.76, 159.67, 149.59, 146.79, 145.07, 139.43, 134.60, 133.04, 131.45, 128.68, 128.47, 128.13, 126.19, 122.10, 119.82, 118.70, 102.87, 99.37, 53.16, 16.61. ESI-MS: m/z 517.5 [M+H]⁺. C₂₉H₂₄N₈O₂ (516.20).

4-((4-(4-((4-cyanophenyl)amino)pyrimidin-4-yl)oxy)-3,5-dimethylphenyl)-1H-1,2,3-triazol-1-yl)methyl)benzenesulfonamide (ZL9).

Recrystallized from EA/PE as a white solid, 73.5% yield, m.p. 290 – 292 °C; ¹H NMR (400 MHz, DMSO-*d*₆) δ 10.06 (s, 1H, NH), 8.62 (s, 1H, triazole-H), 8.40 (d, $J = 5.7$ Hz, 1H, C₆-pyrimidine-H), 7.79 (d, $J = 8.2$ Hz, 2H, Ph-H), 7.64 (s, 2H), 7.56 (d, $J = 8.5$ Hz, 2H, Ph-H), 7.46 (d, $J = 8.1$ Hz, 2H, Ph-H), 7.35 (m, 4H, NH₂, Ph-H), 6.56 (d, $J = 5.6$ Hz, 1H, C₅-pyrimidine-H), 5.70 (d, $J = 11.9$ Hz, 2H, CH₂), 2.05 (s, 6H, 2CH₃). ¹³C NMR (100 MHz, DMSO-*d*₆) δ 169.12, 160.78, 159.66, 149.63, 146.85, 145.08, 144.34, 140.21, 133.03, 131.47, 128.78, 128.64, 126.68, 126.21, 122.20, 119.84, 118.70, 102.86, 99.37, 52.94, 16.61; ESI-MS: m/z 553.3 [M+H]⁺. C₂₈H₂₄N₈O₃S (552.17).

4-((4-(2,6-dimethyl-4-(1-(2-nitrobenzyl)-1H-1,2,3-triazol-4-yl)phenoxy)pyrimidin-2-yl)amino)benzonitrile (ZL10).

Recrystallized from EA/PE as a white solid, 68.3% yield, m.p. 221 – 222 °C; ¹H NMR (400 MHz, DMSO-*d*₆) δ 10.14 (s, 1H, NH), 8.73 (s, 1H, triazole-H), 8.47 (d, $J = 5.7$ Hz, 1H, C₆-pyrimidine-H), 8.31 – 8.20 (m, 2H, Ph-H), 7.82 (d, $J = 7.7$ Hz, 1H, Ph-H), 7.77 – 7.69 (m, 3H, Ph-H), 7.63 (d, $J = 8.4$ Hz, 2H, Ph-H), 7.41 (d, $J = 8.4$ Hz, 2H, Ph-H), 6.64 (d, $J = 5.7$ Hz, 1H, C₅-pyrimidine-H), 5.88 (s, 2H, CH₂), 2.13 (s, 6H, 2CH₃). ¹³C NMR (100 MHz, DMSO-*d*₆) δ 168.98, 160.78, 159.66, 149.65, 148.43, 146.88, 145.06, 138.52, 135.09, 133.00, 131.49, 130.97, 128.58, 126.19, 123.66, 123.28, 122.22, 119.78, 118.68, 102.87, 99.36, 52.51, 16.61. ESI-MS: m/z 519.3 [M+H]⁺. C₂₈H₂₂N₈O₃ (518.18).

4-((4-(2,6-dimethyl-4-(1-(3-nitrobenzyl)-1H-1,2,3-triazol-4-yl)phenoxy)pyrimidin-2-yl)amino)benzonitrile (ZL11).

Recrystallized from EA/PE as a light yellow solid, 65.6% yield, m.p. 226 – 228 °C; ¹H NMR (400 MHz, DMSO-*d*₆) δ 10.14 (s, 1H, NH), 8.63 (s, 1H, triazole-H), 8.47 (d, *J* = 5.6 Hz, 1H, C₆-pyrimidine-H), 8.18 (d, *J* = 8.1 Hz, 1H, Ph-H), 7.80 (t, *J* = 7.5 Hz, 1H, Ph-H), 7.73 (s, 2H, Ph-H), 7.72 – 7.61 (m, 3H, Ph-H), 7.43 (d, *J* = 8.5 Hz, 2H, Ph-H), 7.18 (d, *J* = 7.8 Hz, 1H, Ph-H), 6.64 (d, *J* = 5.6 Hz, 1H, C₅-pyrimidine-H), 6.06 (s, 2H, CH₂), 2.13 (s, 6H, 2CH₃). ¹³C NMR (100 MHz, DMSO-*d*₆) δ 168.97, 160.82, 159.65, 149.70, 147.76, 146.90, 145.07, 143.89, 133.00, 131.51, 129.41, 128.57, 126.19, 124.47, 122.37, 119.82, 118.67, 102.83, 99.34, 52.66, 16.61. ESI-MS: *m/z* 519.3 [M+H]⁺. C₂₈H₂₂N₈O₃ (518.18).

4-((4-(2,6-dimethyl-4-(1-(4-nitrobenzyl)-1H-1,2,3-triazol-4-yl)phenoxy)pyrimidin-2-yl)amino)benzonitrile (ZL12).

Recrystallized from EA/PE as a light yellow solid, 62.7% yield, m.p. 266 – 268 °C; ¹H NMR (400 MHz, DMSO-*d*₆) δ 10.15 (s, 1H, NH), 8.72 (s, 1H, triazole-H), 8.47 (d, *J* = 5.6 Hz, 1H, C₆-pyrimidine-H), 8.28 (d, *J* = 8.3 Hz, 2H, Ph-H), 7.73 (s, 2H, Ph-H), 7.60 (t, *J* = 7.4 Hz, 4H, Ph-H), 7.40 (d, *J* = 8.4 Hz, 2H, Ph-H), 6.65 (d, *J* = 5.6 Hz, 1H, C₅-pyrimidine-H), 5.89 (s, 2H, CH₂), 2.13 (s, 6H, 2CH₃). ¹³C NMR (100 MHz, DMSO-*d*₆) δ 168.97, 160.82, 159.65, 149.70, 147.76, 146.90, 145.07, 143.89, 133.00, 131.51, 129.41, 128.57, 126.19, 124.47, 122.37, 119.82, 118.67, 102.83, 99.34, 52.66, 16.61. ESI-MS: *m/z* 519.3 [M+H]⁺. C₂₈H₂₂N₈O₃ (518.18).

4-((4-(4-(1-benzyl-1H-1,2,3-triazol-4-yl)-2,6-dimethylphenoxy)pyrimidin-2-yl)amino)benzonitrile (ZL13)

Recrystallized from EA/PE as a white solid, 57.2% yield, m.p. 217 – 219 °C; ¹H NMR (400 MHz, DMSO-*d*₆) δ 10.07 (s, 1H, NH), 8.63 (s, 1H, triazole-H), 8.40 (d, *J* = 5.7 Hz, 1H, C₆-pyrimidine-H), 7.65 (d, *J* = 9.7 Hz, 4H, Ph-H), 7.44 (d, *J* = 8.5 Hz, 2H, Ph-H), 7.29 (t, *J* = 7.4 Hz, 2H, Ph-H), 7.23 (d, *J* = 7.0 Hz, 3H, Ph-H), 6.57 (d, *J* = 5.7 Hz, 1H, C₅-pyrimidine-H), 5.76 (s, 2H, CH₂), 2.06 (s, 6H, 2CH₃). ¹³C NMR (100 MHz, DMSO-*d*₆) δ 168.98, 160.79, 159.65, 149.67, 146.88, 145.07, 141.93, 133.28, 133.01, 131.49, 129.09, 128.58, 126.19, 122.32, 119.83, 118.67, 111.45, 102.85, 99.34, 52.92, 16.60. ESI-MS: *m/z* 474.5 [M+H]⁺. C₂₈H₂₃N₇O (473.20).

4-((4-(2,6-dimethyl-4-(1-phenethyl-1H-1,2,3-triazol-4-yl)phenoxy)pyrimidin-2-yl)amino)benzonitrile (**ZL14**).

Recrystallized from EA/PE as a white solid, 64.6% yield, m.p. 167 – 168 °C; ¹H NMR (400 MHz, DMSO-*d*₆) δ 10.14 (s, 1H, NH), 8.55 (s, 1H, triazole-H), 8.47 (d, *J* = 5.6 Hz, 1H, C₆-pyrimidine-H), 7.65 (d, *J* = 9.7 Hz, 4H, Ph-H), 7.44 (d, *J* = 8.5 Hz, 2H, Ph-H), 7.29 (t, *J* = 7.4 Hz, 2H, Ph-H), 7.23 (d, *J* = 7.0 Hz, 3H, Ph-H), 6.65 (d, *J* = 5.6 Hz, 1H, C₅-pyrimidine-H), 4.69 (t, *J* = 7.2 Hz, 2H, CH₂), 3.25 (t, *J* = 7.2 Hz, 2H, CH₂), 2.13 (s, 6H, 2CH₃). ¹³C NMR (100 MHz, DMSO-*d*₆) δ 168.99, 160.74, 159.67, 149.48, 146.20, 145.09, 138.08, 133.02, 131.42, 129.15, 128.90, 127.08, 126.04, 121.73, 119.83, 118.70, 102.87, 99.42, 51.18, 36.09, 16.63. ESI-MS: *m/z* 488.4 [M+H]⁺. C₂₉H₂₅N₇O (487.21).

4-((4-(2,6-dimethyl-4-(1-(2-(thiophen-2-yl)ethyl)-1H-1,2,3-triazol-4-yl)phenoxy)pyrimidin-2-yl)amino)benzonitrile (**ZL15**).

Recrystallized from EA/PE as a light yellow crystal solid, 56.2% yield, m.p. 188–189 °C; ¹H NMR (400 MHz, DMSO-*d*₆) δ 10.14 (s, 1H, NH), 8.54 (s, 1H, triazole-H), 8.47 (d, *J* = 5.6 Hz, 1H, C₆-pyrimidine-H), 7.65 (d, *J* = 13.7 Hz, 4H, Ph-H), 7.51 – 7.38 (m, 3H, thiophene-H, Ph-H), 7.24 (d, *J* = 2.9 Hz, 1H, thiophene-H), 7.01 (dd, *J* = 4.9, 1.2 Hz, 1H, thiophene-H), 6.65 (d, *J* = 5.6 Hz, 1H, C₆-pyrimidine-H), 4.69 (t, *J* = 7.2 Hz, 2H, CH₂), 3.27 (t, *J* = 7.2 Hz, 2H, CH₂), 2.13 (s, 6H, 2CH₃). ¹³C NMR (100 MHz, DMSO-*d*₆) δ 169.00, 160.74, 159.67, 149.49, 146.22, 145.08, 138.28, 133.03, 131.42, 128.88, 128.66, 126.69, 126.05, 122.58, 121.70, 119.85, 118.69, 102.87, 99.41, 50.54, 30.73, 30.48, 16.64; ESI-MS: *m/z* 494.4 [M+H]⁺. C₂₇H₂₃N₇OS (493.17).

2-(4-(4-((2-((4-cyanophenyl)amino)pyrimidin-4-yl)oxy)-3,5-dimethylphenyl)-1H-1,2,3-triazol-1-yl)-N-(4-(methylsulfonyl)phenyl)acetamide (**ZL16**).

Recrystallized from EA/PE as a light yellow solid, 67.5% yield, m.p. 285 – 287 °C; ¹H NMR (400 MHz, DMSO-*d*₆) δ 11.08 (s, 1H, CONH), 10.13 (s, 1H, NH), 8.63 (s, 1H, triazole-H), 8.48 (d, *J* = 5.6 Hz, 1H, C₆-pyrimidine-H), 7.89 (q, *J* = 8.7 Hz, 4H, Ph-H), 7.74 (s, 2H, Ph-H), 7.67 (d, *J* = 8.4 Hz, 2H, Ph-H), 7.45 (d, *J* = 8.5 Hz, 2H, Ph-H), 6.65 (d, *J* = 5.6 Hz, 1H, C₅-pyrimidine-H), 5.50 (s, 2H, CH₂), 3.19 (s, 3H,

CH₃), 2.15 (s, 6H, 2CH₃). ¹³C NMR (100 MHz, DMSO-*d*₆) δ 165.53, 160.74, 159.69, 150.13, 149.49, 146.34, 145.09, 143.36, 135.75, 133.06, 131.48, 128.83, 126.17, 123.51, 119.63, 118.70, 102.91, 94.64, 52.95, 44.23, 16.65. ESI-MS: *m/z* 595.4 [M+H]⁺. C₃₀H₂₆N₈O₄S (594.18).

N-(4-bromophenyl)-2-(4-(4-((2-((4-cyanophenyl)amino)pyrimidin-4-yl)oxy)-3,5-dimethylphenyl)-1*H*-1,2,3-triazol-1-yl)acetamide (**ZL17**).

Recrystallized from EA/PE as a white solid, 58.4% yield, m.p. 239 – 241 °C; ¹H NMR (400 MHz, DMSO-*d*₆) δ 10.68 (s, 1H, CONH), 10.14 (s, 1H, NH), 8.62 (s, 1H, triazole-H), 8.48 (d, *J* = 5.6 Hz, 1H, C₆-pyrimidine-H), 7.74 (s, 2H, Ph-H), 7.68 (d, *J* = 8.5 Hz, 2H, Ph-H), 7.64 – 7.50 (m, 4H, Ph-H), 7.46 (d, *J* = 8.5 Hz, 2H, Ph-H), 6.64 (d, *J* = 5.6 Hz, 1H, C₅-pyrimidine-H), 5.43 (s, 2H, CH₂), 2.15 (s, 6H, 2CH₃). ¹³C NMR (100 MHz, DMSO-*d*₆) δ 169.01, 164.85, 160.73, 159.70, 149.53, 146.32, 145.09, 138.26, 133.06, 132.24, 131.46, 128.78, 126.16, 123.48, 121.68, 119.84, 118.70, 115.92, 102.90, 99.41, 52.91, 16.65. ESI-MS: *m/z* 595.3 [M+H]⁺. C₂₉H₂₃BrN₈O₂ (594.11).

2-(4-(4-((2-((4-cyanophenyl)amino)pyrimidin-4-yl)oxy)-3,5-dimethylphenyl)-1*H*-1,2,3-triazol-1-yl)-*N*-(4-fluorophenyl)acetamide (**ZL18**).

Recrystallized from EA/PE as a white solid, 53.6% yield, m.p. 283 – 286 °C; ¹H NMR (400 MHz, DMSO-*d*₆) δ 10.55 (s, 1H, CONH), 10.07 (s, 1H, NH), 8.55 (s, 1H, triazole-H), 8.40 (d, *J* = 5.6 Hz, 1H, C₆-pyrimidine-H), 7.67 (s, 2H, Ph-H), 7.64 – 7.53 (m, 4H, Ph-H), 7.39 (d, *J* = 8.5 Hz, 2H, Ph-H), 7.13 (t, *J* = 8.8 Hz, 2H, Ph-H), 6.57 (d, *J* = 5.6 Hz, 1H, C₅-pyrimidine-H), 5.35 (s, 2H, CH₂), 2.08 (s, 6H, 2CH₃). ¹³C NMR (100 MHz, DMSO-*d*₆) δ 169.01, 164.57, 160.73, 159.92, 159.69, 157.54, 149.52, 146.31, 145.09, 135.29, 133.06, 131.46, 128.78, 126.16, 123.48, 121.59, 121.51, 119.85, 118.69, 116.12, 115.89, 102.89, 99.42, 52.83, 16.65. ESI-MS: *m/z* 535.3 [M+H]⁺. C₂₉H₂₃FN₈O₂ (534.19).

Methyl 2-(4-(4-((2-((4-cyanophenyl)amino)pyrimidin-4-yl)oxy)-3,5-dimethylphenyl)-1*H*-1,2,3-triazol-1-yl)acetate (**ZL19**).

Recrystallized from EA/PE as a light yellow solid, 66.4% yield, m.p.: 221-224°C; ¹H NMR (400 MHz, DMSO-*d*₆) δ 10.13 (s, 1H, NH), 8.59 (s, 1H, triazole-H), 8.47 (d,

$J = 5.6$ Hz, 1H, C₆-pyrimidine-H), 7.72 (s, 2H, Ph-H), 7.66 (d, $J = 8.5$ Hz, 2H, Ph-H), 7.44 (d, $J = 8.5$ Hz, 2H, Ph-H), 6.64 (d, $J = 5.6$ Hz, 1H, C₅-pyrimidine-H), 5.51 (s, 2H, CH₂), 3.76 (s, 3H, CH₃), 2.14 (s, 6H, 2CH₃). ¹³C NMR (100 MHz, DMSO-*d*₆) δ 168.99, 168.14, 160.75, 159.68, 149.62, 146.49, 145.09, 133.04, 131.51, 128.58, 126.19, 123.17, 119.82, 118.69, 102.89, 99.41, 53.09, 51.00, 16.63; ESI-MS: m/z 456.5 [M+H]⁺. C₂₄H₂₁N₇O₃ (455.17).

Methyl 3-(4-(4-((2-((4-cyanophenyl)amino)pyrimidin-4-yl)oxy)-3,5-dimethylphenyl)-1H-1,2,3-triazol-1-yl)propanoate (ZL20).

Recrystallized from EA/PE as a white solid, 57.8% yield, m.p. 145 – 146 °C; ¹H NMR (400 MHz, DMSO-*d*₆) δ 10.07 (s, 1H, NH), 8.53 (s, 1H, triazole-H), 8.40 (d, $J = 5.6$ Hz, 1H, C₆-pyrimidine-H), 7.67 – 7.54 (m, 4H, Ph-H), 7.36 (d, $J = 8.5$ Hz, 2H, Ph-H), 6.57 (d, $J = 5.6$ Hz, 1H, C₅-pyrimidine-H), 4.60 (t, $J = 6.7$ Hz, 2H, CH₂), 3.56 (s, 3H, CH₃), 3.00 (t, $J = 6.7$ Hz, 2H, CH₂), 2.06 (s, 6H, 2CH₃). ¹³C NMR (100 MHz, DMSO-*d*₆) δ 171.25, 168.99, 160.76, 159.67, 149.52, 146.27, 145.07, 133.03, 131.44, 128.79, 126.10, 122.03, 119.82, 118.68, 102.86, 99.39, 52.18, 45.88, 34.16, 16.63. ESI-MS: m/z 470.3 [M+H]⁺. C₂₅H₂₃N₇O₃ (469.19).

Methyl 4-(4-(4-((2-((4-cyanophenyl)amino)pyrimidin-4-yl)oxy)-3,5-dimethylphenyl)-1H-1,2,3-triazol-1-yl)butanoate (ZL21).

Recrystallized from EA/PE as a white solid, 61.3% yield, m.p. 111 – 113 °C; ¹H NMR (400 MHz, DMSO-*d*₆) δ 10.14 (s, 1H, NH), 8.63 (s, 1H, triazole-H), 8.47 (d, $J = 5.6$ Hz, 1H, C₆-pyrimidine-H), 7.71 (s, 2H, Ph-H), 7.64 (d, $J = 8.5$ Hz, 2H, Ph-H), 7.43 (d, $J = 8.5$ Hz, 2H, Ph-H), 6.65 (d, $J = 5.6$ Hz, 1H, C₅-pyrimidine-H), 4.48 (t, $J = 6.9$ Hz, 2H, CH₂), 3.60 (s, 3H, CH₃), 2.39 (t, $J = 7.3$ Hz, 2H, CH₂), 2.22 – 2.13 (m, 2H, CH₂), 2.13 (s, 6H, 2CH₃). ¹³C NMR (100 MHz, DMSO-*d*₆) δ 172.96, 169.00, 160.77, 159.67, 149.52, 146.47, 145.07, 133.02, 131.42, 128.88, 126.13, 121.79, 119.79, 118.70, 102.88, 99.38, 51.89, 49.25, 30.64, 25.55, 16.63. ESI-MS: m/z 484.5 [M+H]⁺. C₂₆H₂₅N₇O₃ (483.20).

4.2. In vitro anti-HIV assay

The target compounds were evaluated for their activity and cytotoxicity against WT HIV-1 (strain HIV-IIIB), double RT mutant strain HIV-1 IIIB (RES056 and

F227L/V106A), five single RT mutant strain HIV-1 IIIB (L100I, K103N, E138K, Y181C, Y188L), and HIV-2 (strain ROD) utilizing the MTT method in MT-4 cells described previously.^{3,28} Firstly, the stock solutions ($10 \times$ final concentrations) of test compounds were added in 25 μ L volumes to two series of triplicate wells to allow simultaneous evaluation of their effects on mock-and HIV-infected cells. Using a Biomek 3000 robot (Beckman instruments, Fullerton, CA), the prepared concentrations of these compounds were diluted to five-fold serially in flat-bottomed 96-well microtiter trays, including untreated control HIV-1 and mock-infected cells for each sample.

HIV-1 (IIIB), HIV-1 (RES056, F227L/V106A, L100I, K103N, E138K, Y181C and Y188L) or HIV-2 (ROD) stock (50 mL at 100-300 CCID₅₀) (50% cell culture infectious dose) or culture medium was added to either the infected or mock-infected wells of the microtiter tray. Mock-infected cells were utilized to evaluate the effect of test compounds on normal cells in order to evaluate their cytotoxicity. Exponentially growing MT-4 cells were centrifuged for 5 min at 1000 rpm and the supernatant was discarded. The MT-4 cells were resuspended at 6×10^5 cells/mL, and then transferred 50 μ L volumes to the microtiter tray wells. After infecting the MT-4 cells for five days, the survivability of mock-and HIV-infected cells was inspected spectrophotometrically by the MTT assay, suggesting the activity of test compounds. The 50% cytotoxic concentration (CC₅₀) was defined as the concentration of the test compound that reduced the absorbance (OD₅₄₀) of the mock-infected control sample by 50%. The concentration achieving 50% protection from the cytopathic effect of the virus in infected cells was defined as the 50% effective concentration (EC₅₀).

4.3. HIV-1 RT inhibition assay

A HIV-1 reverse transcriptase (RT) assay kit produced by Roche was selected for the RT inhibition assay. All the reagents for performing the RT reaction start from the kit and the particular ELSIA procedures for RT inhibition assay was carried out following the description in the kit protocol.²⁹ Briefly, the reaction mixture containing template/primer complex, viral nucleotides (dNTPs) and RT in the incubation buffer with or without inhibitors was incubated for 1 hour at 37°C. After that, the reaction

mixture was transferred to a streptavidine-coated microtiter plate and incubated for another 1 hours at 37°C to make sure retranscriptional cDNA chain that consisted biotin-labeled dNTPs bound to streptavidine. Then removed un-bound dNTPs using washing buffer and added anti-DIG-POD working solution. After incubation for 1hour at 37°C, the DIG-labeled dNTPs incorporated in cDNA were bound to the anti-DIG-POD antibody. The unbound anti-DIG-PODs were removed and the peroxidesubstrate (ABST) solution was added to the MTPs. A colored reaction proceeds during cleavage of the substrate catalyzed by POD. The absorbance of the sample was determined at OD 405 nm using a microtiter plate ELISA reader. The percentage inhibitory activity of RT inhibitors was calculated by formula as given below:

$$\% \text{Inhibition} = \frac{[\text{OD value with RT but without inhibitors} - \text{OD value with RT and inhibitors}]}{[\text{OD value with RT and inhibitors} - \text{OD value without RT and inhibitors}]}$$

The IC₅₀ values corresponded to the concentrations of the inhibitors required to inhibit biotin-dUTP incorporation by 50%.

4.4. Molecular simulation

The molecule for docking built using standard bond lengths and angles from Sybyl-X 2.0/Base Builder and was optimized using the Tripos force field for 1000-generations until the maximum derivative of energy became 0.005 kcal/(mol*A). Charges were computed and added according to Gasteiger-Huckel parameters. The published three dimensional crystal structures of RT complexes (HIV-1 WT RT (PDB: 2ZD1) and K103N RT (PDB: 3MEG)) were retrieved from the Protein Data Bank and were used for the docking experiment by means of surflex-docking module of Sybyl-X 2.0. The protein was prepared by removing the ligand, water molecules, and other unnecessary small molecules from the crystal structure of the ligand HIV-1 RT complex before docking; polar hydrogen atoms and charges were added to the protein. After the protomol was generated, the optimized molecule was surflex-docked into the binding pocket of NNRTIs, with therelevant parameters set as defaults. Top-scoring pose was shown by the software of PyMOL version 1.5 (www.pymol.org.). The secondary structure of RT is shown in surface, and only the

key residues for interactions with the inhibitor were shown in sticks and labeled. The potential hydrogen bonds were presented by dashed lines.

AUTHOR INFORMATION

Corresponding Authors

*C.P.: e-mail, christophe.pannecouque@rega.kuleuven.be; phone, 32-(0)16-332171;

*P.Z.: e-mail, zhanpeng1982@sdu.edu.cn; phone, 086-531-88382005;

*X.L.: e-mail, xinyongl@sdu.edu.cn; phone, 086-531-88380270.

Notes

The authors declare no competing financial interest.

ACKNOWLEDGMENTS

Financial support from the National Natural Science Foundation of China (NSFC No. 81273354), Key Project of NSFC for International Cooperation (No. 81420108027), Young Scholars Program of Shandong University (YSPSDU No. 2016WLJH32, to P.Z.), Key Research and Development Project of Shandong Province (Grant 2017CXGC1401), Major Project of Science and Technology of Shandong Province (No. 2015ZDJS04001) and KU Leuven (GOA 10/014) is gratefully acknowledged. We thank K. Erven, K. Uyttensprot and C. Heens for technical assistance with the HIV assays.

References

1. K. Das, E. Arnold, *Curr. Opin. Virol.*, 3 (2013) 111-118.
2. J. Guilleumont, L. Geeraert, J. Heeres, P.J. Lewi, *Wiley - VCH Verlag GmbH & Co. KGaA*, 2010.
3. D.W. Wright, S. S. Kashif, D.F. Gianni, P.V. Coveney, *J. Am. Chem. Soc.*, 134 (2012) 12885-12888.
4. F. Caterina, G. Sandra, B. Stefania, H. Paul, C. Bruno, P. Marco, D.A. Meri, F. Isabella, N. Vito, R. Anna, *J. Med. Chem.*, 48 (2005) 7153-7165.
5. D. Kang, Z. Wang, H. Zhang, G. Wu, T. Zhao, Z. Zhou, Z. Huo, B. Huang, D. Feng, X. Ding, *ACS Med. Chem. Lett.*, 9 (2018) 370.
6. E.B. Lansdon, K.M. Brendza, H. Magdeleine, W. Ruth, M. Susmith, J. Debi, B. Gabriel, K. Nilima, L. Xiaohong, *J. Med. Chem.*, 53 (2010) 4295-4299.
7. D. Kang, Z. Fang, Z. Li, B. Huang, H. Zhang, X. Lu, H. Xu, Z. Zhou, X. Ding, D. Daelemans, *J. Med. Chem.*, 59 (2016) 7991-8007.
8. S. Rik, *Expert Opin. Pharmacother.*, 14 (2013) 1087-1096.

9. N. Listed, *Prescrire Int.*, 21 (2012) 262-265.
10. M.P.D. Béthune, *Antiviral Res.*, 85 (2010) 75-90.
11. P. Zhan, C. Pannecouque, C.E. De, X. Liu, *J. Med. Chem.*, 59 (2015) 2849-2878.
12. Zhan, P. Chen, X. Li, D. Fang, Z.D. Clercq, E. Liu, Xinyong, *Med. Res. Rev.*, 33 (2013) E1-E72.
13. X. Zuo, Z. Huo, D. Kang, G. Wu, Z. Zhou, X. Liu, P. Zhan, *Expert Opin Ther Pat.*, 2018 Apr; 28(4):299-316.
14. Y. Yang, D. Kang, L.A. Nguyen, Z.B. Smithline, C. Pannecouque, P. Zhan, X. Liu, T.A. Steitz, *Elife*, 2018 Jul 25;7. pii: e36340.
15. L. Won-Gil, K.M. Frey, G.M. Ricardo, K.A. Spasov, B. Mariela, K.S. Anderson, W.L. Jorgensen, *ACS Med. Chem. Lett.*, 5 (2014) 1259-1262.
16. T. Xingtao, Q. Bingjie, W. Zhiyuan, W. Xiaofeng, L. Hong, S.L. Morris-Natschke, C. Chin Ho, J. Shibo, L. Kuo-Hsiung, X. Lan, *J. Med. Chem.*, 53 (2010) 8287-8297.
17. L. Won-Gil, G.M. Ricardo, K.M. Frey, K.A. Spasov, B. Mariela, K.S. Anderson, W.L. Jorgensen, *J. Am. Chem. Soc.*, 135 (2013) 16705-16713.
18. Z. Zhou, T. Liu, D. Kang, Z. Huo, G. Wu, D. Daelemans, C.E. De, C. Pannecouque, P. Zhan, X. Liu, *Org Biomol Chem.*, 2018 Feb 7;16(6):1014-1028.
19. L. Wang, Y. Tian, W. Chen, H. Liu, P. Zhan, D. Li, H. Liu, E.C. De, C. Pannecouque, X. Liu, *Eur. J. Med. Chem.*, 85 (2014) 293-303.
20. X. Wang, B. Huang, X. Liu, Z. Peng, *Drug Discov Today.*, 2016 Jan;21(1):118-132.
21. D. Kang, H. Zhang, Z. Zhou, B. Huang, L. Naesens, Z. Peng, X. Liu, *Bioorg. Med. Chem. Lett.*, 26 (2016) 5182-5186.
22. G. Ping, S. Lin, J. Zhou, L. Xiao, Z. Peng, X. Liu, *Expert Opin Drug Discov.*, 2016 Sep;11(9): 857-871.
23. Y. Tian, Z. Liu, J. Liu, B. Huang, D. Kang, H. Zhang, E.C. De, D. Daelemans, C. Pannecouque, K.H. Lee, *Eur J Med Chem.*, 151 (2018) 339-350.
24. S.X. Gu, H. Qiao, Y.Y. Zhu, Q.C. Shu, H. Liu, X.L. Ju, E.D. Clercq, J. Balzarini, C. Pannecouque, *Bioorg. Med. Chem.*, 23 (2015) 6587-6593.
25. C.M. Bailey, T.J. Sullivan, I. Pinar, T.R. Julian, C. Raymond, R.C. Juliana, M. Ebrahim, J. William, H. Roger, K.S. Anderson, *J. Med. Chem.*, 56 (2013) 3959-3968.
26. C. Xuebing, W. Youzhi, X. Jinyi, Y. Hequan, L. Aijun, H. Yue, *Org. Biomol. Chem.*, 13 (2015) 9186-9189.
27. S.S. Carroll, D.B. Olsen, C.D. Bennett, L. Gotlib, ., D.J. Graham, J.H. Condra, A.M. Stern, J.A. Shafer, L.C. Kuo, *J Biol Chem.*, 1993 Jan 5;268(1):276-281.
28. P. Christophe, D. Dirk, D.C. Erik, *Nat. Protoc.*, 3 (2008) 427-434.
29. K. Suzuki, B.P. Craddock, N. Okamoto, T. Kano, R.T., *J. Virol. Methods*, 44 (1993) 189-198.

View Article Online
DOI: 10.1039/C9OB00032A